BIOCHEMISTRY
including biophysical chemistry & molecular biology

ARTICLE

pubs.acs.org/biochemistry

Indolequinone Inhibitors of NRH:Quinone Oxidoreductase 2. Characterization of the Mechanism of Inhibition in both Cell-Free and Cellular Systems

Chao Yan,[†] Marine Dufour,[‡] David Siegel,[†] Philip Reigan,[†] Joe Gomez,[†] Biehuoy Shieh,[†] Christopher J. Moody,[*,‡] and David Ross[*,†]

[†]Department of Pharmaceutical Sciences, School of Pharmacy, University of Colorado Denver, Aurora, Colorado 80045, United States

[‡]School of Chemistry, University of Nottingham, University Park, Nottingham NG7 2RD, U.K.

Supporting Information

ABSTRACT: We describe a series of indolequinones as efficient mechanism-based inhibitors of NRH:quinone oxidoreductase 2 (NQO2) for use either in cellular or cell-free systems. Compounds were designed to be reduced in the active site of the enzyme leading to loss of a substituted phenol leaving group and generation of a reactive iminium electrophile. Inhibition of NQO2 activity was assessed in both cell-free systems and the human leukemia K562 cell line. Inhibition of recombinant human NQO2 by the indolequinones was NRH-dependent, with kinetic parameters characteristic of mechanism-based inhibition and partition ratios as low as 2.0. Indolequinones inhibited NQO2 activity in K562 cells at nanomolar concentrations that did not inhibit NQO1 and were nontoxic to cells. Computation-based molecular modeling simulations demonstrated favorable conformations of indolequinones positioned directly above and in parallel with the isoalloxazine ring of FAD, and mass spectrometry extended our previous finding of adduction of the FAD in the active site of NQO2 by an indolequinone-derived iminium electrophile to the wider series of indolequinone inhibitors. Modeling combined with biochemical testing identified key structural parameters for effective inhibition, including a 5-aminoalkylamino side chain. Hydrogen bonding of the terminal amine nitrogen in the aminoalkylamino side chain was found to be critical for the correct orientation of the inhibitors in the active site. These indolequinones were irreversible inhibitors and were found to be at least 1 order of magnitude more potent than any previously documented competitive inhibitors of NQO2 and represent the first mechanism-based inhibitors of NQO2 to be characterized in cellular systems.

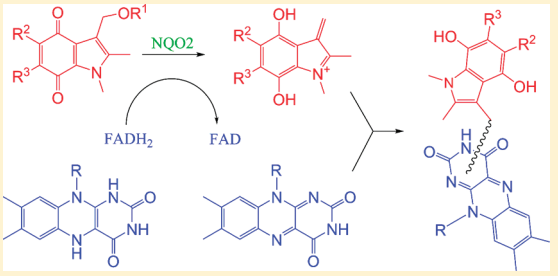

There are two quinone reductases that occur in mammalian systems, NAD(P)H:quinone oxidoreductase 1 (NQO1, EC 1.6.99.2) and NRH:quinone oxidoreductase 2 (NQO2, EC 1.10.99.2). NQO1 was originally characterized by Ernster and Navazio[1,2] and was probably identical to an enzyme isolated by Martius a few years earlier.[3,4] Interestingly, NQO2 was cloned and fully characterized by Jaiswal et al.[5] but as highlighted by Zhao et al.[6] was also found to be identical to a flavoprotein isolated 30 years earlier.[7] Both NQO1 and NQO2 are homodimeric flavoproteins, containing one FAD site per monomer, that utilize pyridine nucleotide cofactors to catalyze the direct two-electron reduction of a broad range of quinone substrates.[6,8,9] However, NQO2 differs from NQO1 in that it utilizes dihydronicotinamide riboside (NRH) instead of NAD(P)H as the cofactor. In addition, in comparison to NQO1, which is usually strongly expressed in solid tumors,[10] higher levels of NQO2 expression are found in red blood cells[11] and in leukemias.[12] With respect to quinone substrates, NQO2 has been suggested to preferentially reduce *o*-quinones derived from catecholamines and estrogen, which has led to its proposed involvement in neurodegenerative diseases and breast cancer.[13,14] NQO2 has been shown to reduce numerous antitumor quinones in vitro, including mitomycin C,[15] RH1,[16] and the HSP90 inhibitor 17AAG,[17] while the antitumor activity of CB1954, a non-quinone dinitrobenzamide-containing compound currently in clinical trials, relies on targeted activation by NQO2 via nitroreduction.[18]

The identification of inhibitors for NQO2 has generated considerable interest. Despite structural similarities between NQO2 and NQO1, commonly used NQO1 inhibitors such as dicoumarol[19] and ES936[20] are extremely poor inhibitors of NQO2, while conversely, inhibitors of NQO2 such as resveratrol and quercetin have been shown to selectively inhibit NQO2 but not NQO1.[21−23] Previous studies have shown that resveratrol,[21,22] quercetin,[23] chloroquine,[11,24] and melatonin[9,25] can inhibit the catalytic activity of NQO2 but do so reversibly. In addition to inhibiting NQO2, these compounds have also been

Received: February 26, 2011
Revised: May 10, 2011
Published: June 30, 2011

shown to inhibit other enzymes and have direct antioxidant activities. Most recently, NQO2 has been found to be the major non-kinase target of imatinib in leukemia cells,[12,26] suggesting it may play an as yet uncharacterized role in leukemia and/or imatinib pharmacodynamics. All of these studies point to an emerging role for NQO2 in diverse physiological and disease process, but one major obstacle in defining the role of NQO2 in complex cellular systems has been the absence of potent and specific inhibitors of the enzyme. We have recently examined the structural requirements for selective inhibition of NQO2 relative to NQO1[27] and proposed a novel mechanism of inhibition involving flavin adduction. In this study, we have characterized a series of indolequinones as mechanism-based inhibitors of NQO2 that can be utilized in both cell-free and cellular systems. In addition, we have utilized molecular modeling in combination with biochemical studies and mass spectrometry to define the structural parameters of this indolequinone series that are necessary for effective inhibition of NQO2.

MATERIALS AND METHODS

Materials. NADH, FAD, 2,6-dichlorophenolindophenol (DCPIP), 3-(4,5-dimethylthiazol-2-yl)-2,5-diphenyltetrazolium bromide (MTT), menadione, resveratrol, chloroquine, quercetin, and melatonin were obtained from Sigma (St. Louis, MO). Imatinib mesylate was purchased from LC laboratories (Woburn, MA). The indolequinones 5-(4-aminobutyl)amino-1,2-dimethyl-3-[(4-nitrophenoxy)methyl]indole-4,7-dione (**1**), 5-(4-aminobutyl)amino-1,2-dimethyl-3-[(2,4,6-trifluorophenoxy)methyl]indole-4,7-dione (**2**), 6-(4-aminobutyl)amino-1,2-dimethyl-3-[(2,4,6-trifluorophenoxy)methyl]indole-4,7-dione (**3**), 5-(3-aminopropyl)amino-1,2-dimethyl-3-[(2,4,6-trifluorophenoxy)methyl]indole-4,7-dione (**4**), 5-(3-dimethylamino)propylamino-1,2-dimethyl-3-[(2,4,6-trifluorophenoxy)methyl]indole-4,7-dione (**5**), 6-(3-dimethylamino)propylamino-1,2-dimethyl-3-[(2,4,6-trifluorophenoxy)methyl]indole-4,7-dione (**6**), 5-(3-dimethylamino)propylmethylamino-1,2-dimethyl-3-[(2,4,6-trifluorophenoxy)methyl]indole-4,7-dione (**7**), 5-(3-dimethylamino)propylamino-1,2-dimethyl-3-(phenoxymethyl)indole-4,7-dione (**8**), and 5-(3-dimethylamino)propylamino-1,2-dimethyl-3-(hydroxymethyl)-indole-4,7-dione (**9**) were synthesized using published methods[27] except that indolequinones **3** and **6** were prepared as described in the Supporting Information. Recombinant human NQO1 (rhNQO1) was purified from *Escherichia coli* using Cibacron blue affinity chromatography as previously described.[28] Recombinant human NQO2 (rhNQO2) was purchased from Sigma, dissolved in 250 mM sucrose, and stored at −80 °C. Dihydronicotinamide riboside (NRH) was prepared from NADH using previously reported methods.[16,29]

Cell Lines. Human leukemia cell line K562 was obtained from ATCC (Manassas, VA) and grown in complete RPMI1640 medium supplemented with 4 mM L-glutamine, 10% (v/v) fetal bovine serum, 100 units/mL penicillin, and 100 μg/mL streptomycin. Cells were maintained in a humidified incubator containing 5% carbon dioxide at 37 °C.

Inhibitor Screening for NQO2. Mechanism-based inactivation of NQO2 by this indolequinone series was assayed using purified human recombinant NQO2 (rhNQO2). In these reactions (final volume of 0.5 mL), rhNQO2 (4 μg/mL) was incubated with 0.1−10.0 μM indolequinone in the absence and presence of 0.2 mM NRH in 50 mM potassium phosphate buffer (pH 7.4) containing 5 μM FAD, 125 mM NaCl, and 1 mg/mL bovine serum albumin at room temperature. After 5 min, a 50 μL aliquot was removed and diluted 50-fold in stop buffer [50 mM potassium phosphate buffer (pH 7.4) containing 250 mM sucrose, 5 μM FAD, 0.1% (v/v) Tween 20, and 0.25 mg/mL MTT]. An aliquot (960 μL) of the mixture was then transferred to a cuvette and mixed with 200 μM NRH and 10 μM menadione (final volume of 1 mL), and the linear increase in absorbance was monitored spectrophotometrically at 550 nm for 2 min at room temperature. NQO2 activity was measured as NRH-dependent menadione reductase activity using MTT as the final electron acceptor.[23]

Inhibitor Characterization. Partition ratios for inactivation of rhNQO2 by the indolequinones that demonstrated mechanism-based inhibition were determined by using the methods described above except that the indolequiones and rhNQO2 were incubated in the presence of 0.2 mM NRH for 15 min, with defined molar ratios of indolequinone to rhNQO2 monomer (active sites) (range from 0.25:1 to 120:1). The percent of activity remaining for each concentration was then plotted versus the molar ratio; a straight line was generated using linear regression and extrapolated, and the *x*-intercept of the line represents the partition ratio (number of molecules of inhibitor metabolized to inactivate one molecule of enzyme).[30]

The concentration- and time-dependent inactivation of NQO2 by the selected indolequinone **1** and **5** was examined to confirm mechanism-based inhibition. For these studies, inactivation of NQO2 by indolequinone **1** or **5** was performed at 4 °C in a reaction system (final volume of 1 mL) containing 50 mM potassium phosphate buffer (pH 7.4), 0.1% Tween 20, 125 mM NaCl, 200 μM NRH, 5 μM FAD, and 4 μg/mL rhNQO2. Indolequinones **1** and **5** were then added independently (final concentration from 0 to 2 μM), and at the indicated time points, an aliquot (40 μL) was removed and diluted 100-fold in stop buffer [50 mM potassium phosphate buffer (pH 7.4) containing 250 mM sucrose, 5 μM FAD, 200 μM NRH, and 0.1% (v/v) Tween 20] and frozen immediately in liquid nitrogen. NQO2 activity was then measured at room temperature in samples (960 μL) supplemented with 10 μM menadione and 0.1 mg/mL MTT (final volume of 1 mL), and the linear increase in absorbance at 550 nm was monitored for 3 min. The data generated were analyzed using the Kitz and Wilson plot,[31] and the K_i and k_{inact} values were calculated accordingly.

Comparison of Indolequinones with Known Competitive Inhibitors of NQO2. The ability of various compounds to inhibit NQO2 was compared in an assay adapted for a 96-well format using resazurin as the NQO2 substrate. A 100 μL portion of the reaction mixture was set up for each drug concentration containing 50 mM potassium phosphate buffer (pH 7.4), 1 mg/mL BSA, 125 mM NaCl, 5 μM FAD, 200 μM NRH, and 20 ng of NQO2. Drugs were then introduced at final concentrations from 0.0025 to 250 μM and the mixtures incubated at room temperature for 5 min; 10 μL of the resazurin stock solution was then added into each well to achieve a final concentration of 15 μM. The fluorescence of reduced resazurin was then monitored with 530 nm excitation and 590 nm emission for 5 min using a Molecular Devices SpectraMax fluorescence plate reader. The rate of change in fluorescence per minute was calculated and the NQO2 activity remaining expressed as a percentage of the DMSO-treated control.

Inactivation of NQO2 and NQO1 in K562 Cells. The inhibition of NQO2 activity in K562 cells by these indolequinones was determined using the following procedure. K562 cells

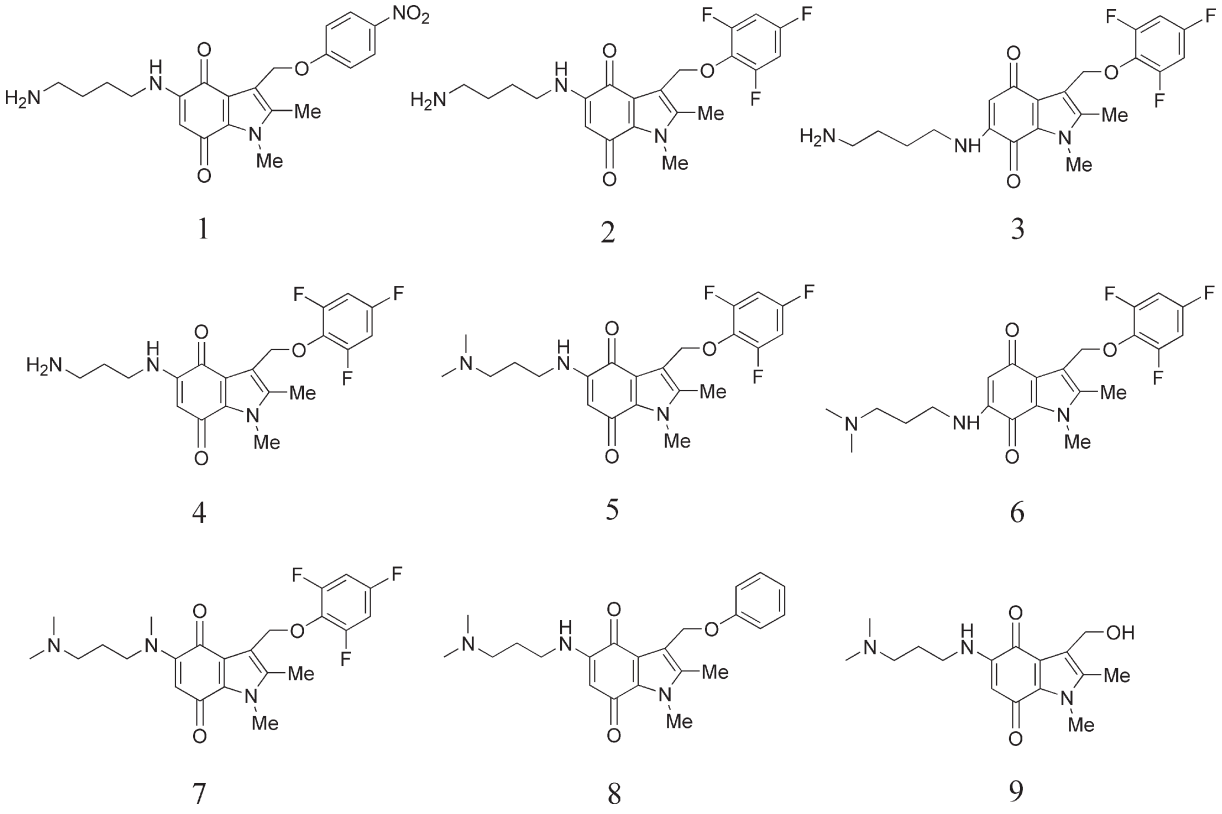

Figure 1. Chemical structures of the indolequinones.

(3×10^6) were treated with various concentrations of inhibitors for 15 min in 1 mL of complete medium, after which the medium was removed by centrifugation (1500 rpm for 3 min), and cells were washed twice with cold PBS. Cells were then resuspended in 25 mM Tris buffer (pH 7.4) containing 250 mM sucrose and 5 μM FAD and sonicated on ice. The protein concentrations of sonicates were determined by the method of Lowry.[32] NQO2 activity was determined using NRH-dependent CB1954 metabolism.[23] For these studies, 25 μL of cell sonicates was mixed with 25 μL of 25 mM Tris-HCl buffer (pH 7.4) containing 400 μM NRH and 100 μM CB1954 and allowed to react at room temperature for 15 min. The reaction was then stopped by the addition of 50 μL of cold acetonitrile; the mixture was centrifuged at 13K rpm (4 °C), and 25 μL of the supernatant was removed and analyzed for CB1954 metabolism by high-performance liquid chromatography (HPLC) as previously described.[23] The amount of CB1954 consumed (proportional to NQO2 activity) was then calculated for each sample. NQO2 activity was normalized to protein content, and the results were expressed as a percentage of the DMSO-treated control. NQO1 activity of cell sonicates was determined by measuring NADH-dependent reduction of DCPIP in 1 mL reaction mixtures at room temperature. Briefly, an aliquot of sonicate was added to 50 mM potassium phosphate buffer containing 0.1% Tween 20, 200 μM NADH, and 40 μM DCPIP, and the linear decrease in absorbance was measured at 600 nm over 1 min.

Growth Inhibition Assay. Growth inhibition of K562 cells was assessed using the MTT colorimetric assay.[33] For these studies, K562 cells were seeded at a density of 5×10^4 cells/well in 96-well plates, in triplicate for each compound, and then allowed to recover for 1 h. Cells were then treated with the appropriate concentration of indolequinone (0−5000 nM) in complete medium. After 72 h, 10 μL of complete medium containing MTT (5 mg/mL) was added to each well and incubated for an additional 4 h. Plates were then centrifuged at 1000 rpm for 5 min; the medium was removed, and DMSO (100 μL) was then added to each well to dissolve the crystalline formazan product derived from the cellular metabolism of MTT. Optical density was determined at 550 nm using a Molecular Devices Thermomax microplate reader. The IC_{50} value was defined as the concentration of indolequinone that resulted in a 50% reduction in cell number compared to the DMSO-treated control, determined from semilogarithmic plots of the percentage of control versus indolequinone concentration.

Molecular Docking of the Indolequinone Ligands into NQO2. All simulations were performed with Discovery Studio version 2.5.5 (Accelrys Inc., San Diego, CA). The 1.8 Å structure of human NQO2 cocrystallized with indolequinone **1** (Protein Data Bank entry 3O73) has been resolved by our group and deposited in the Protein Data Bank. The CHARMm force field[34] was applied to the NQO2 structure to represent the protonation state of the protein at physiological pH. The binding site was defined as whole residues within an interface 12 Å radius subset encompassing the FAD cofactor. LigandFit[35] was used for the molecular docking of indolequinones **1**−**9** into the binding site of NQO2. Fifty structural outputs were specified, and the identification of a docked conformation was followed by a minimization (1000 iterations) using the conjugate gradient method to a convergence of 0.001 kcal/mol. The Poisson−Boltzmann method was used to calculate binding energy, with a nonbonded list radius of 14 Å.[36] The conformations for each docked complex were ranked on the basis of binding energy and

interactions examined. The top-ranked poses were subsequently chosen on the basis of binding energies and interactions known to be essential for efficient mechanism-based inhibition, including hydrogen bonding and π-stacking between the indolequinone and FAD cofactor.[20,27,37,38]

HPLC and Mass Spectrometry Analysis of FAD Adducts. Indolequinone-inactivated human recombinant NQO2 protein for HPLC and MS analysis was prepared by incubating 25 μg of rhNQO2 with a 10-fold molar excess of indolequinones in 25 mM potassium phosphate buffer (pH 7.4, final volume of 40 μL) in the presence or absence of 0.5 mM NRH. Reactions were stopped after 10 min by the addition of 60 μL of ice-cold methanol to denature NQO2 and release FAD. Precipitated protein was removed by centrifugation (13000 rpm for 5 min at 4 °C), and 50 μL of the supernatant was then loaded onto a C_{18} reverse-phase HPLC column [Luna C18(2), 5 μm, 250 mm × 4.6 mm, Phenomenex, Torrance, CA] and eluted at a rate of 1 mL/min with a mobile phase of 10 mM ammonium acetate (A) and 100% acetonitrile (B) with a linear gradient from 5 to 50% B over 15 min using a detection wavelength of 260 nm. For LC−MS analysis, rhNQO2 was inactivated and FAD extracted as described above and then concentrated under vacuum (SpeedVac, Savant AES-1000), and 8 μL of the sample was introduced into an Agilent 1100 capillary HPLC system utilizing a 1.0 mm × 150 mm Grace Vydac C_{18} MS column (218MS5115) and a mobile phase of 10 mM ammonium acetate (A) and 10 mM ammonium acetate in acetonitrile (B) with a linear gradient from 5 to 60% B over 10 min at a flow rate of 50 μL/min. Spectra were recorded on a Waters QTOFII mass spectrometer in positive mode, scanning from m/z 200 to 1500 using a 1 s scan time.

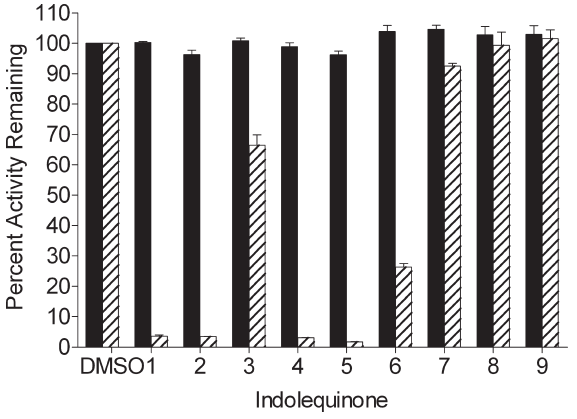

Figure 2. NRH-dependent inhibition of NQO2 by indolequinones. Purified rhNQO2 was incubated with 1 μM indolequinones in the absence (filled bars) or presence (hatched bars) of NRH, and after 5 min, an aliquot was removed and assayed for NQO2 catalytic activity. Results are expressed as percentages of NQO2 activity remaining compared to DMSO-treated controls. Reaction conditions are described in Materials and Methods. Results represent the mean ± standard deviation of three independent determinations.

RESULTS

Indolequinones. A series of indolequinones were selected for this study varying in both the 5- and 6-substituents and the leaving group at the 3-position. The 5- and 6-substituents were chosen to examine the effect of structural variations in the side chain on inhibition of NQO2 and the impact of 5- versus 6-substitutions. Compounds were designed to have either very good leaving groups at the indole 3-position, such as 4-nitrophenoxy and 2,4,6-trifluorophenoxy, or very poor leaving groups under physiological conditions (3-phenoxy and 3-hydroxy). Chemical structures of the indolequinones used in these studies are shown in Figure 1.

NRH-Dependent NQO2 Inhibition by Indolequinones. The ability of indolequinones to inhibit recombinant human NQO2 protein was examined in the presence and absence of the cofactor NRH. For these studies, rhNQO2 was incubated with

Table 1. Biochemical and Physical Characterization of the Indolequinones

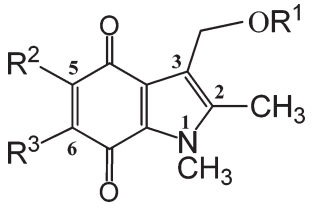

compd	R^1	R^2	R^3	rhNQO2 inhibition at 1 μM[a]	partition ratio[b]	IC_{50}[c] for K562 cells (μM)	binding energy[d] (kcal/mol)
1	4-NO_2-C_6H_4	$NH_2(CH_2)_4NH$	H	96%	2.0	>10	−21.6
2	2,4,6-F_3-C_6H_2	$NH_2(CH_2)_4NH$	H	96%	2.0	>10	−30.2
3	2,4,6-F_3-C_6H_2	H	$NH_2(CH_2)_4NH$	33%	14.0	>10	−18.0
4	2,4,6-F_3-C_6H_2	$NH_2(CH_2)_3NH$	H	97%	2.1	>10	−21.7
5	2,4,6-F_3-C_6H_2	$(CH_3)_2N(CH_2)_3NH$	H	98%	2.1	>10	−26.5
6	2,4,6-F_3-C_6H_2	H	$(CH_3)_2N(CH_2)_3NH$	73%	3.7	>10	−12.8
7	2,4,6-F_3-C_6H_2	$(CH_3)_2N(CH_2)_3N(CH_3)$	H	5%	74	>10	−13.1
8	C_6H_5	$(CH_3)_2N(CH_2)_3NH$	H	NI[e]	NI[e]	>10	−34.4
9	H	$(CH_3)_2N(CH_2)_3NH$	H	NI[e]	NI[e]	>10	−25.9

[a] rhNQO2 inhibition by 1 μM indolequinone was also graphed (Figure 2). [b] The partition ratio for each compound was determined as described in Materials and Methods. [c] IC_{50} values in K562 cells were determined using the MTT assay. [d] Binding energies in the form of ΔG were calculated from molecular modeling simulations. [e] No inhibition.

dx.doi.org/10.1021/bi2002967 |*Biochemistry* 2011, 50, 6678–6688

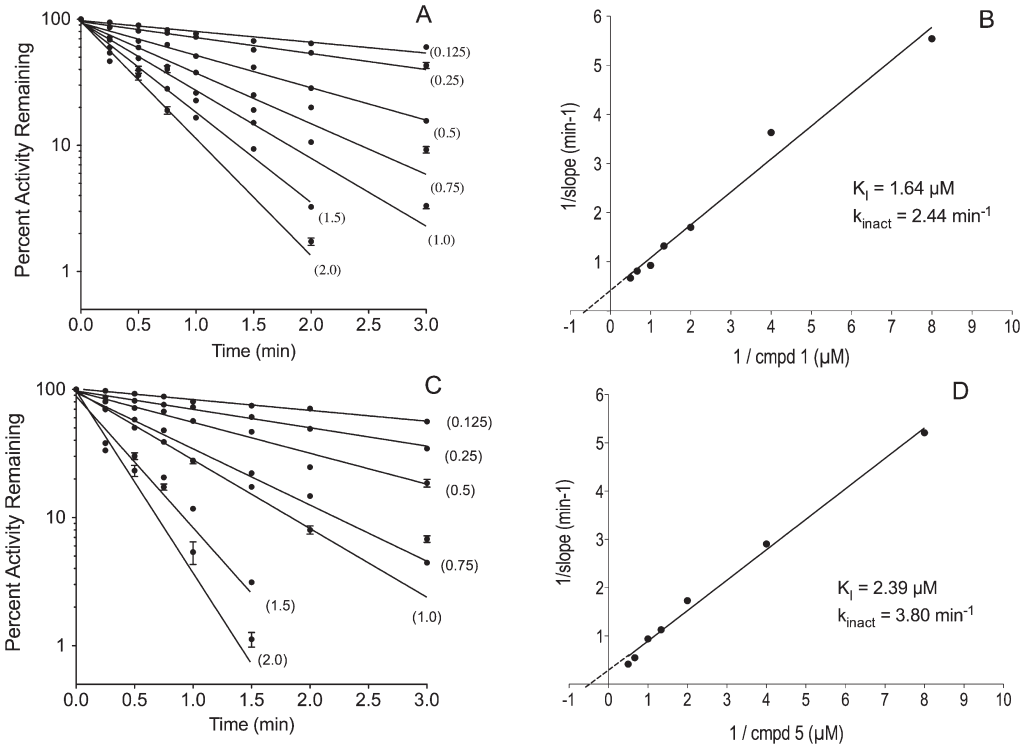

Figure 3. Kinetic analysis of the inhibition of NQO2 by indolequinones. Concentration- and time-dependent inhibition of rhNQO2 by indolequinones **1** (A) and **5** (C). Results are expressed as the percentage of NQO2 activity remaining compared to DMSO-treated controls. Results represent the mean ± standard deviation of three independent determinations. Best-fit lines were derived from nonlinear regression analysis. The resultant Kitz−Wilson plots are shown for indolequinones **1** (B) and **5** (D).

indolequinones in the presence and absence of NRH for 5 min, after which a sample of the reaction mixture was removed and diluted and NQO2 activity was measured spectrophotometrically (550 nm) using NRH-dependent menadione reduction coupled to MTT reduction.[23] The incubation of **1**, **2**, **4**, and **5** (1 μM) with NRH and rhNQO2 resulted in greater than 95% inhibition of NQO2 catalytic activity (Figure 2 and Table 1), and this inactivation was dependent upon NRH, suggestive of mechanism-based inhibition. These data demonstrated that variations in the 5-position amino alkyl chain length, $(CH_2)_n$ where n = 3 (compounds **4** and **5**) or n = 4 (compounds **1** and **2**), as well as substitutions on the terminal amine (compound **5**) were tolerated and resulted in marked NQO2 inhibition. However, aminoalkylamino substitutions at the 6-position (compounds **3** and **6**) resulted in compounds that were much poorer inhibitors when compared to indolequinones substituted at the 5-position. No inhibition of rhNQO2 was observed with indolequinones **7**−**9** in the presence or absence of NRH. Data for compound **7** illustrate that branching of the proximal nitrogen in the aminoalkylamino chain is not optimal for inhibition, while the studies with compounds **8** and **9** demonstrated that a leaving group is required at the 3-position for inhibition. Inhibition of NQO2 by the indolequinones appeared to be irreversible because desalting of the indolequinone-inhibited protein using the Millipore Microcon Molecular Cutoff device did not result in recovery of enzyme activity (data not shown). To determine if these compounds could also inhibit the related enzyme NQO1, we incubated rhNQO1 with indolequinones (1 μM) in the presence and absence of NADH, and in these studies, no inhibition of NQO1 was detected.[27]

Kinetic Analysis of NQO2 Inhibition by Indolequinones. Indolequinones **1** and **5** were selected for kinetic analysis because they were the most efficient NQO2 inhibitors. The inactivation of NQO2 by both indolequinones was very rapid, and consequently, the time dependence and concentration dependence of the inhibition kinetics were determined at 4 °C. As shown in Figure 3, the inhibition of NQO2 by compound **1** (A) and **5** (C) was both time- and concentration-dependent. K_i and k_{inact} were determined from Kitz−Wilson plots (Figure 3B,D) as described previously.[31]

Determination of the Partition Ratio. The partition ratio for a mechanism-based inhibitor is the number of catalytic cycles required to inactivate one molecule of enzyme;[30] therefore, the lower the partition ratio, the more efficient the inhibitor. To compare the efficiency of NQO2 inhibition, the partition ratio for each indolequinone that demonstrated NRH-dependent NQO2 inhibition was determined (Table 1). Partition ratios of approximately 2 were determined for inactivation of NQO2 by indolequinones **1**, **2**, **4**, and **5**, indicating that these indolequinones were extremely efficient mechanism-based inhibitors of NQO2. The 6-aminoalkylamino compounds, **3** and **6**, had partition ratios of 14.0 and 3.7, respectively, displaying less efficient mechanism-based inhibition of NQO2 when compared to those of their 5-aminoalkylamino counterparts. Partition ratios for indolequinones **8** and **9** were not determined because they did not inhibit NQO2.

Potency of Indolequinone Inhibitors Relative to Previously Characterized Competitive Inhibitors of NQO2. The ability of indolequinones to inactivate NQO2 was compared with that of previously reported competitive NQO2 inhibitors using a 96-well based assay as described in Materials and Methods.

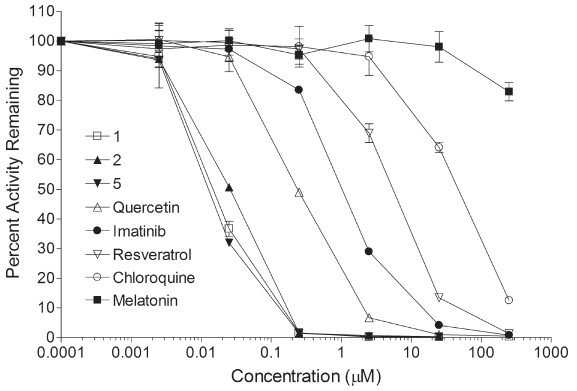

Figure 4. Comparison of indolequinones with known inhibitors of NQO2. Indolequinones **1**, **2**, and **5** were compared with previously reported NQO2 inhibitors quercetin, imatinib, resveratrol, chloroquine, and melatonin for their ability to inhibit rhNQO2 activity in a cell-free system. Inhibition reaction and activity measurement were conducted as described in Materials and Methods. Results are expressed as percentages of NQO2 activity remaining compared to DMSO-treated controls. Results represent the mean ± standard deviation of three independent determinations.

Indolequinones **1**, **2**, and **5** were considerably more potent as inhibitors of NQO2 than either quercetin, imatinib, resevratrol, chloroquine, or melatonin (Figure 4). A molar comparison showed inhibition more potent by at least 1 order of magnitude with the indolequinone inhibitors than with other compounds used.

Inhibition of NQO2 Activity by Indolequinones in K562 Cells. The ability of indolequinones **1**, **2**, **4**, and **5** to inhibit NQO2 activity in cells was examined in human leukemia cell line K562 (Figure 5). K562 cells were chosen because they contain very high levels of NQO2 activity and protein and only trace levels of NQO1 activity and protein (Figure 5, inset). For these studies, K562 cells were treated with increasing concentrations of indolequinones for 15 min, after which the cells were collected and NQO2 (Figure 5A) and NQO1 (Figure 5B) activities were measured. Results from these studies demonstrated that these indolequinones could enter cells and efficiently inhibit NQO2. Greater than 95% of NQO2 activity could be inhibited following treatment with indolequinones (Figure 5A). Importantly, NQO1 activity was not affected under the same conditions (Figure 5B). These data demonstrated that aminoalkyl-substituted indolequinones have very good selectivity for NQO2 over NQO1 in cells.

Growth Inhibition by Indolequinones in K562 Cells. Growth inhibition studies were performed in K562 cells. Cells were treated for 72 h with various concentrations of indolequinones. The IC_{50} values were calculated from the survival curve and are reported in Table 1. All of the indolequinones tested have an IC_{50} values of >10 μM (the highest concentration tested). These results indicate that these indolequinones are nontoxic to K562 cells at concentrations that result in greater than 95% inhibition of NQO2 activity.

Molecular Modeling of Indolequinones into NQO2. Molecular docking simulations were performed for indolequinones **1**−**9** in the active site of NQO2 with the anionic form of the reduced FAD cofactor that represents the physiological situation in which quinone encounters reduced FAD.[8,39] High-ranking binding conformations of the indolequinones in the active site of NQO2 were identified and are shown in Figure 6 (**1**−**3**, **5**, and **7**)

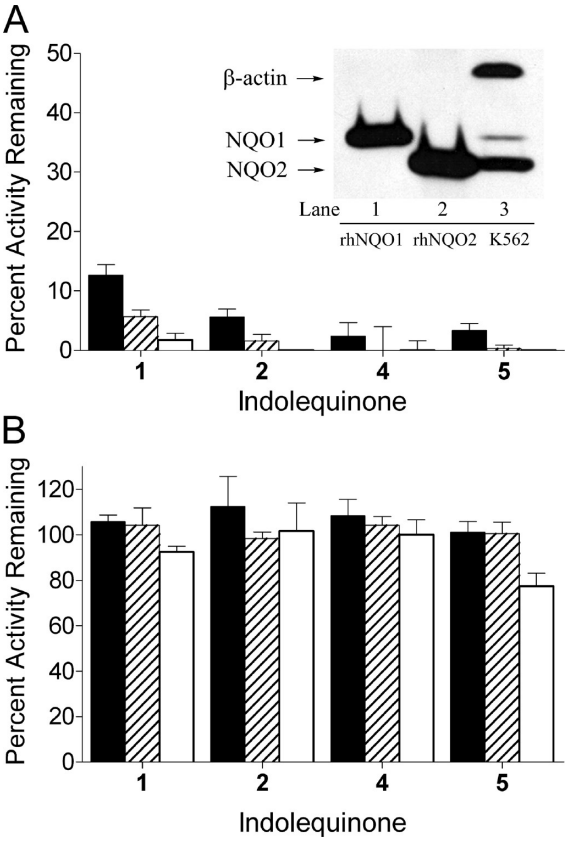

Figure 5. Selective inhibition of NQO2 by indolequinones in K562 cells. K562 human leukemia cells were treated with indolequinones **1**, **2**, **4**, and **5** (100−500 nM) for 15 min, after which the cells were recovered and NQO2 and NQO1 catalytic activities were measured as described in Materials and Methods. Results are expressed as the percent activity remaining compared to DMSO-treated controls. (A) Percent NQO2 activity remaining following indolequinone treatment. (B) Percent NQO1 activity remaining following indolequinone treatment. Filled columns, 100 nM; striped columns, 250 nM; open columns, 500 nM. Results represent the mean ± standard deviation of three independent determinations. The inset shows immunoblot analysis demonstrating NQO1 and NQO2 protein expression in K562 cells: lane 1, rhNQO1 standard (10 ng); lane 2, rhNQO2 standard (10 ng); lane 3, K562 sonicate (20 μg).

and Figure S1 of the Supporting Information (**4**, **6**, **8**, and **9**). The binding energies corresponding to the selected conformation for each complex were calculated and are listed in Table 1. The conformations of the inhibitors (**1**−**7**) with the indolequinone system stacked in parallel above the isoalloxazine ring of FAD resulted in more favorable binding energies, which could be attributed to the optimal aromatic $\pi-\pi$ interactions between the indolequinone ring and the reduced isoalloxazine ring system of FAD.[40,41] Indolequinones **8** and **9** have high binding energies (Table 1) but are not inhibitors because of the absence of an efficient leaving group. The overall conformations of potent inhibitors **1** (Figure 6A), **2** (Figure 6B), **4** (Figure S1A of the Supporting Information), and **5** (Figure 6D) in the active site of NQO2 were very similar. As observed in the cocrystallized structure,[27] the indolequinone ring was aligned parallel to the isoalloxazine ring of FAD and the C7 carbonyl of the quinone moiety was positioned directly above N5 of the FAD, allowing the efficient transfer of a hydride from the FAD during

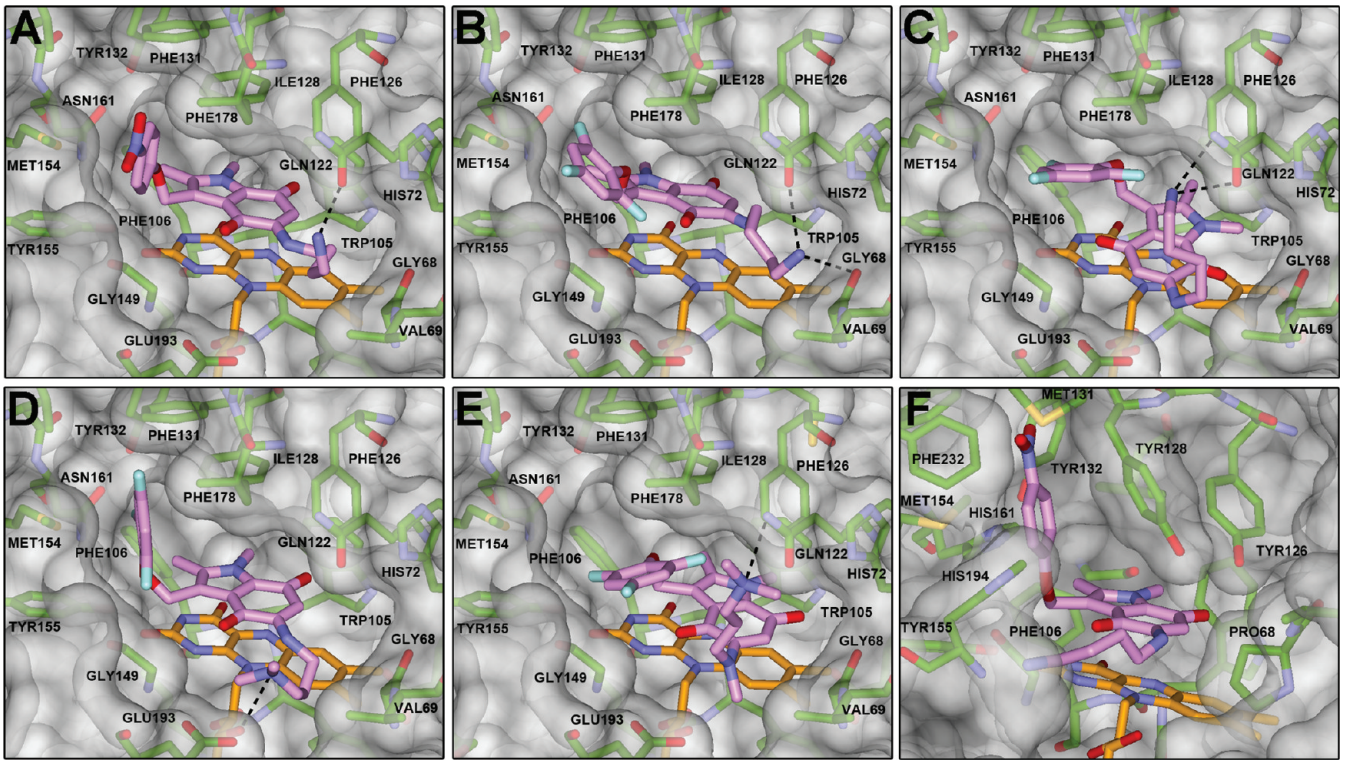

Figure 6. Structural frames from molecular docking simulations of the indolequinone ligands in the active site of NQO2 and NQO1. (A–E) Representations of **1** (A), **2** (B), **3** (C), **5** (D), and **7** (E) in the quinone form (stick display style; carbon atoms colored salmon) in the reduced FAD (stick display style; carbon atoms colored yellow) site of NQO2; key amino acids (stick display style; carbon atoms colored green); and hydrogen bond contacts between the terminal amine of the aminoalkylamino chain and the active site (black dashed line) are displayed. (F) Molecular docking of indolequinone **1** into the active site of NQO1.

reduction.[8,39] The hydrophobic interaction between the indole 2-methyl and residues Phe178 and Phe106 also contributes favorably to the binding energy. These studies also revealed the importance of the interaction between the terminal amine of the aminoalkylamino side chain and the NQO2 active site, which further contributed to the binding energy. The hydrogen bond formed between the terminal amine of the aminoalkylamino side chain and either Gln122, Glu193, or FAD (Figure 6 and Figure S1 of the Supporting Information, black dotted line) at the edge of the binding pocket acts as an anchor that appears to stabilize the binding of the indolequinone in the active site after reduction. The aminoalkylamino substitution at the 6-position (**3** and **6**) results in steric hindrance between the indolequinone and the active site (Figure 6C and Figure S1B of the Supporting Information), making them less efficient inhibitors than the 5-substituted analogues (Figure 6A,D). Incorporating a proximal *N*-methyl branch into the aminoalkylamino side chain[7] hinders the accessibility of the indolequinone to the active site and affected alignment with the FAD (Figure 6E). Consequently, **7** was predicted to be ineffective as an inhibitor of NQO2, which was confirmed by biochemical testing (Figure 2).

Modeling also provided an explanation of the inability of the indolequinone NQO2 inhibitors to inhibit NQO1. The active site of NQO1 is more constrained than NQO2, and the bulky aminoalkylamino at the 5-position blocked entrance of the inhibitors into the NQO1 active site (Figure 6F). The impaired accessibility of the indolequinone inhibitors to the active site of NQO1 relative to NQO2 is shown in Figure 6 using indolequinone **1** as an example.

MS Analysis. Our previous data using compound **1** suggested a novel mechanism of inhibition of NQO2 by the indolequinones involving FAD adduction.[27] To confirm and extend these observations, we examined three additional compounds using ESI-LC–MS. To determine whether the indolequinones were adducted to the noncovalently bound FAD cofactor, we incubated the rhNQO2 protein with indolequinones in the presence and absence of NRH, and the liberated FAD was then analyzed using HPLC and ESI-LC–MS for potential indolequinone-derived adducts. HPLC analysis of FAD extracted from NQO2 following incubation with indolequinone **5** and NRH clearly showed a decrease in the parent FAD peak with the appearance of a new, slightly more hydrophobic peak when compared to incubations performed in the absence of NRH (Figure 7A). LC–MS analysis (positive mode) of the new peak gave the spectrum shown in Figure 7B (MH^+ m/z 1075.35; detailed fragmentation analysis reported in Figure S2 of the Supporting Information). The mass spectrum confirms the presence of a **5** iminium–FAD adduct (FAD, m/z 785, and the reactive iminium intermediate of **5**, m/z 288) and suggests the formation of the hydroquinone form of the iminium–FAD adduct (Scheme 1). To confirm adduction of FAD by the series of indolequinones, these experiments were extended to indolequinones **4** (Figure 7C and Figure S3 of the Supporting Information) and **2** (Figure 7D and Figure S4 of the Supporting Information). In these studies, iminium–FAD adducts could be detected that differ in molecular weight because of the 5-position aminoalkylamino side chain with all indolequinone NQO2 inhibitors tested, demonstrating the generality of this

dx.doi.org/10.1021/bi2002967 |*Biochemistry* 2011, 50, 6678–6688

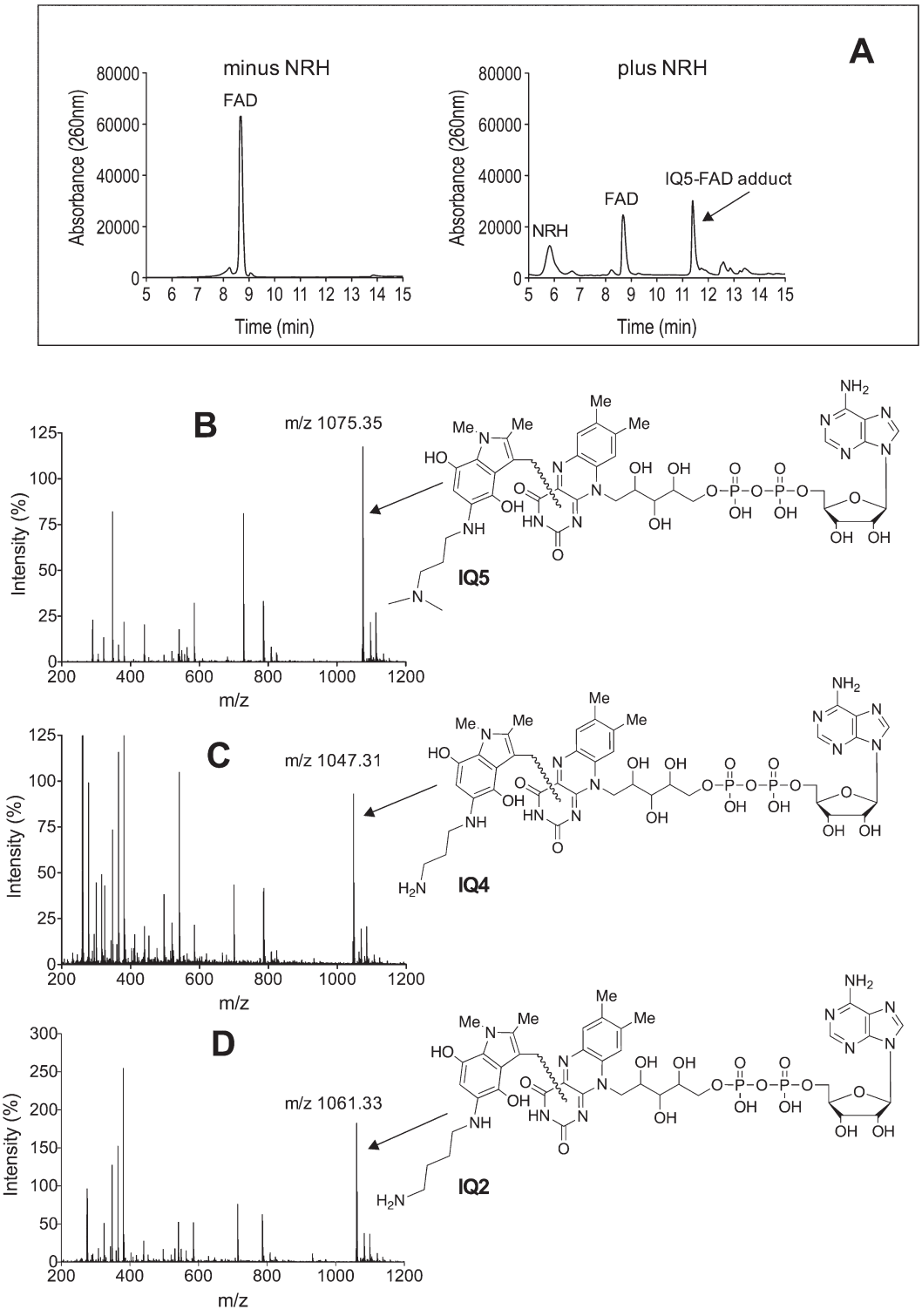

Figure 7. HPLC and LC−MS analysis of the adduction of the FAD cofactor in NQO2 by indolequinones. Incubation of NQO2 with indolequinone in the presence of NRH results in indolequinone adduction of FAD. (A) HPLC analysis (260 nm) of FAD extracted from NQO2 following incubation with indolequinone **5** in the absence (left) and presence (right) of NRH. ESI-LC−MS analyses of FAD adducts obtained from incubation with NQO2 and NRH are also shown for indolequinones **5** (B), **4** (C), and **2** (D). Detailed fragmentation analyses of the FAD adducts are shown in the Supporting Information (Figures S2−S4, respectively).

mechanism. Detailed fragmentation analyses of iminium−FAD adducts generated from indolequinones **5**, **4**, and **2** are shown in the Supporting Information (Figures S2−S4, respectively).

■ DISCUSSION

Several structurally diverse compounds have been shown to be competitive inhibitors of NQO2, including the natural products

dx.doi.org/10.1021/bi2002967 |*Biochemistry* 2011, 50, 6678–6688

Scheme 1. Proposed Mechanism of FAD Adduction by the Indolequinone Inhibitors of NQO2

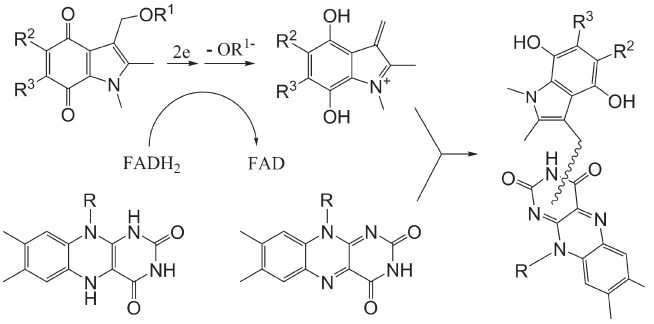

resveratrol,[21,22] quercetin,[23] casimiroin,[42] and melatonin[9,25] and the drugs choloroquine[11,24] and imatinib.[12,26] The indolequinones we have developed were designed to undergo NQO2-mediated reduction to the hydroquinone form and subsequent elimination of a leaving group from the (indol-3-yl) methyl position. This results in the generation of a reactive iminium ion that directly alkylates within the NQO2 active site, resulting in the irreversible inhibition of NQO2 enzymatic activity. An important measure of mechanism-based inhibition is the requirement for the catalytic step to occur prior to inactivation of the enzyme. The inhibition of rhNQO2 activity by this series of indolequinones was therefore monitored in the presence and absence of NRH to determine if the inhibition of rhNQO2 was mechanism-based. Indolequinones **1**−**6** demonstrated NRH-dependent NQO2 inhibition, which supports mechanism-based inactivation. In addition, inhibition of NQO2 by indolequinones was time- and concentration-dependent, which is characteristic of mechanism-based inhibitors. Moreover, compounds **8** and **9**, which are NQO2 substrates but have a poor leaving group at the 3-position and therefore could not generate an iminium intermediate, were not inhibitors of NQO2, suggesting that reduction and expulsion of the leaving group are prerequisites for the mechanism-based inhibition of NQO2. The indolequinone inhibitors of NQO2 were at least 1 order of magnitude more potent than previously characterized competitive inhibitors quercetin, imatinib, chloroquine, resveratrol, and melatonin.

Structural requirements for effective inhibition of NQO2 were examined and found to include an aminoalkylamino side chain at the 5-position. Compounds in which the aminoalkyl chain terminated in either an unsubstituted amino group (**1**, **2**, and **4**) or a dimethyl-substituted amino group (**5**) were efficient inhibitors of NQO2. Compounds with aminoalkylamino substitutions at the 6-position (**3** and **6**) were not efficient mechanism-based inhibitors of NQO2. As discussed above, a good leaving group at the 3-position (either 4-nitrophenoxy or 4-trifluorophenoxy) that allows generation of a reactive iminium electrophile following enzymatic reduction is essential for efficient NQO2 inhibition by these compounds, and because indolequinones **8** and **9** do not meet this requirement, they were not inhibitors of NQO2. Our molecular modeling simulations suggested tight binding between the inhibitors and the NQO2 active site. The terminal amine nitrogen in the aminoalkylamino side chain was shown to be critical for the binding of the indolequinones by forming hydrogen bonds with Gln122 or Glu193 or FAD and providing an anchor point for the indolequinones in the active site. The molecular modeling simulations also provided a possible explanation for the inefficiency of **3** and **6** in inhibiting NQO2 compared to **2** and **5**. As shown in Figure 6 and Figure S1 of the Supporting Information, indolequinones with a side chain located at the 5-position are positioned in parallel above the isoalloxazine rings and oriented such that the quinone is directly above N5 in FAD. In contrast, indolequinones with a side chain located at the 6-position do not orient themselves with the quinone ring positioned directly above N5 of FAD, resulting in less efficient inhibition of NQO2. If the side chain is branched at the nitrogen proximal to the quinone ring (see indolequinone **7**), then docking of the compound into the active site of NQO2 is blocked. This hypothesis was confirmed as indolequinone **7** was a very poor inhibitor of NQO2 in biochemical studies.

Although based on an identical indolequinone backbone like the previously reported series of NQO1 inhibitors,[37,43] the compounds reported in these studies exhibited selectivity for inhibition of NQO2. In a cell-free system, rhNQO1 was only slightly inhibited by indolequinones using concentrations 1 order of magnitude greater than those required for complete inhibition of NQO2.[27] Studies in K562 cells demonstrated that NQO1 activity was not affected despite >95% inhibition of NQO2 activity after treatment for 15 min with indolequinones (Figure 5). The selective inhibition of NQO2 over NQO1 could be attributed to the bulky aminoalkylamino substituent at the 5-position, which blocks entrance of the indolequinones into the NQO1 active site (Figure 6F). The NQO2 active site is wider and more hydrophobic than that of NQO1 and could adequately accommodate these larger indolequinones. We cannot exclude the possibility that other flavoproteins could also be inhibited by the indolequinones. However, this seems unlikely given the requirement for two-electron reduction to release the reactive iminium, the need for an active site that will accommodate the indolequinone in an optimal binding orientation, and the specificity of these indolequinones for NQO2 relative to the structurally related NQO1.

Analysis of the active site of NQO2 using molecular modeling simulations demonstrated a lack of amino acids in the active site suitable for covalent adduction by electrophiles, and we were unable to detect the adduction of amino acids following incubation of either indolequinone **1** or **5** with NQO2 and NRH using LC−MS analysis. In contrast, adducts could readily be detected using the indolequinone ES936 and the related enzyme NQO1 as we have previously reported.[20] Our previously published data[27] indicated that nucleophilic sites in FAD were potential adduction sites, and we confirmed these data and extended them to three other additional indolequinone inhibitors, indicating the generality of the FAD adduction mechanism for this series of inhibitors. ESI-LC−MS confirmed the presence of a FAD adduct generated from the iminium electrophile obtained after reduction of the indolequinone and loss of the leaving group consistent with the proposed scheme for activation (Scheme 1). These FAD adducts are relatively unstable once FAD is extracted from NQO2 (data not shown), and unequivocal assignment of the structure of the FAD adducts formed will require further studies most probably using biological NMR.

A unique feature of NQO2 is that it is usually expressed at very low levels in human solid tumors but is expressed at higher levels in leukemias[6] and could be a potential therapeutic target. NQO2 has been shown to be the major non-kinase target of imatinib in leukemias, raising the intriguing possibility that NQO2 may contribute to leukemia cell growth or alternatively may act as a sink for imatinib altering its pharmacodynamics. Our

data indicate that indolequinones were nontoxic to K562 cells at the concentrations where complete NQO2 inhibition was achieved, and although this was not the major goal of our study, it does suggest that inhibition of NQO2 alone is not sufficient to cause leukemia cell death. However, it is possible that NQO2 inhibition may have a synergistic effect with Bcr-Abl inhibition in the presence of imatinib, or alternatively that NQO2 inhibition by indolequinone could potentiate imatinib toxicity by increasing the concentration of free drug. Both genetic and pharmacologic approaches are currently underway in our laboratory in an effort to fully understand the role of NQO2 in leukemias and in imatinib pharmacology.

In summary, we have generated and characterized a series of indolequinone compounds as mechanism-based inhibitors of NQO2 in cell-free and cellular systems. The indolequinones are the most effective inhibitors of NQO2 described to date, and utilizing modeling, biochemical studies, and mass spectrometry, we have characterized both their mechanism of inhibition and structural parameters required for effective inhibition of NQO2.

■ ASSOCIATED CONTENT

Supporting Information. Structural frames from the molecular docking simulations and mass spectrometry data for some of the indolequinones and the methods for the preparation of indolequinones **3** and **6**. This material is available free of charge via the Internet at http://pubs.acs.org.

■ AUTHOR INFORMATION

Corresponding Author

*D.R. (biology): phone, (303) 724-7265; fax, (303) 724-7266; e-mail, david.ross@ucdenver.edu. C.J.M. (chemistry): phone, +44 115 846 8500; fax, +44 115 951 3564; e-mail, c.j.moody@nottingham.ac.uk.

Author Contributions

C.Y. and M.D. contributed equally to this work.

Funding Sources

This work was funded in part by National Institutes of Health Grant R21 HL095995.

Notes

C.J.M., D.R., and D.S. are cofounders and stockholders in QGenta Inc., which holds an option to license molecules described in this article.

■ ABBREVIATIONS

NQO1, NADH:quinone oxidoreductase 1; NQO2, NRH:quinone oxidoreductase 2; NRH, nicotinamide riboside; MTT, 3-(4,5-dimethylthiazol-2-yl)-2,5-diphenyltetrazolium bromide; ESI-LC−MS, electrospray ionization liquid chromatography−mass spectrometry.

■ REFERENCES

(1) Ernster, L., and Navazio, F. (1958) Soluble diaphorase in animal tissues. *Acta Chem. Scand. 12*, 595–602.

(2) Ernster, L., Ljunggren, M., and Danielson, L. (1960) Purification and some properties of a highly dicumarol-sensitive liver diaphorase. *Biochem. Biophys. Res. Commun. 2*, 88–92.

(3) Martius, C. (1954) [The place of vitamin K1 in respiratory chain; preliminary report.]. *Biochem. Z. 326*, 26–27.

(4) Ernster, L. (1987) DT-diaphorase: A historical review. *Chem. Scr. 27A*, 1–13.

(5) Jaiswal, A. K., Burnett, P., Adesnik, M., and McBride, O. W. (1990) Nucleotide and deduced amino acid sequence of a human cDNA (NQO2) corresponding to a second member of the NAD(P)H:quinone oxidoreductase gene family. Extensive polymorphism at the NQO2 gene locus on chromosome 6. *Biochemistry 29*, 1899–1906.

(6) Zhao, Q., Yang, X. L., Holtzclaw, W. D., and Talalay, P. (1997) Unexpected genetic and structural relationships of a long-forgotten flavoenzyme to NAD(P)H:quinone reductase (DT-diaphorase). *Proc. Natl. Acad. Sci. U.S.A. 94*, 1669–1674.

(7) Liao, S., Dulaney, J. T., and Williams-Ashman, H. G. (1962) Purification and properties of a flavoprotein catalyzing the oxidation of reduced ribosyl nicotinamide. *J. Biol. Chem. 237*, 2981–2987.

(8) Bianchet, M. A., Faig, M., and Amzel, L. M. (2004) Structure and mechanism of NAD[P]H:quinone acceptor oxidoreductases (NQO). *Methods Enzymol. 382*, 144–174.

(9) Vella, F., Ferry, G., Delagrange, P., and Boutin, J. A. (2005) NRH:quinone reductase 2: An enzyme of surprises and mysteries. *Biochem. Pharmacol. 71*, 1–12.

(10) Siegel, D., and Ross, D. (2000) Immunodetection of NAD(P)H:quinone oxidoreductase 1 (NQO1) in human tissues. *Free Radical Biol. Med. 29*, 246–253.

(11) Graves, P. R., Kwiek, J. J., Fadden, P., Ray, R., Hardeman, K., Coley, A. M., Foley, M., and Haystead, T. A. (2002) Discovery of novel targets of quinoline drugs in the human purine binding proteome. *Mol. Pharmacol. 62*, 1364–1372.

(12) Bantscheff, M., Eberhard, D., Abraham, Y., Bastuck, S., Boesche, M., Hobson, S., Mathieson, T., Perrin, J., Raida, M., Rau, C., Reader, V., Sweetman, G., Bauer, A., Bouwmeester, T., Hopf, C., Kruse, U., Neubauer, G., Ramsden, N., Rick, J., Kuster, B., and Drewes, G. (2007) Quantitative chemical proteomics reveals mechanisms of action of clinical ABL kinase inhibitors. *Nat. Biotechnol. 25*, 1035–1044.

(13) Fu, Y., Buryanovskyy, L., and Zhang, Z. (2008) Quinone reductase 2 is a catechol quinone reductase. *J. Biol. Chem. 283*, 23829–23835.

(14) Gaikwad, N. W., Yang, L., Rogan, E. G., and Cavalieri, E. L. (2009) Evidence for NQO2-mediated reduction of the carcinogenic estrogen ortho-quinones. *Free Radical Biol. Med. 46*, 253–262.

(15) Jamieson, D., Tung, A. T., Knox, R. J., and Boddy, A. V. (2006) Reduction of mitomycin C is catalysed by human recombinant NRH:quinone oxidoreductase 2 using reduced nicotinamide adenine dinucleotide as an electron donating co-factor. *Br. J. Cancer 95*, 1229–1233.

(16) Yan, C., Kepa, J. K., Siegel, D., Stratford, I. J., and Ross, D. (2008) Dissecting the role of multiple reductases in bioactivation and cytotoxicity of the antitumor agent 2,5-diaziridinyl-3-(hydroxymethyl)-6-methyl-1,4-benzoquinone (RH1). *Mol. Pharmacol. 74*, 1657–1665.

(17) Siegel, D., Reigan, P., Guo, W., and Ross, D. (2007) The metabolism of antitumor quinones by NRH:quinone oxidoreductase 2 (NQO2). In *Proceedings of the American Association for Cancer Research*, American Association for Cancer Research, Los Angeles.

(18) Knox, R. J., Jenkins, T. C., Hobbs, S. M., Chen, S., Melton, R. G., and Burke, P. J. (2000) Bioactivation of 5-(aziridin-1-yl)-2,4-dinitrobenzamide (CB 1954) by human NAD(P)H quinone oxidoreductase 2: A novel co-substrate-mediated antitumor prodrug therapy. *Cancer Res. 60*, 4179–4186.

(19) Hollander, P. M., and Ernster, L. (1975) Studies on the reaction mechanism of DT diaphorase. Action of dead-end inhibitors and effects of phospholipids. *Arch. Biochem. Biophys. 169*, 560–567.

(20) Winski, S. L., Faig, M., Bianchet, M. A., Siegel, D., Swann, E., Fung, K., Duncan, M. W., Moody, C. J., Amzel, L. M., and Ross, D. (2001) Characterization of a mechanism-based inhibitor of NAD(P)H:quinone oxidoreductase 1 by biochemical, X-ray crystallographic, and mass spectrometric approaches. *Biochemistry 40*, 15135–15142.

(21) Buryanovskyy, L., Fu, Y., Boyd, M., Ma, Y., Hsieh, T. C., Wu, J. M., and Zhang, Z. (2004) Crystal structure of quinone reductase 2 in complex with resveratrol. *Biochemistry 43*, 11417–11426.

(22) Wang, Z., Hsieh, T. C., Zhang, Z., Ma, Y., and Wu, J. M. (2004) Identification and purification of resveratrol targeting proteins using

immobilized resveratrol affinity chromatography. *Biochem. Biophys. Res. Commun. 323*, 743–749.

(23) Wu, K., Knox, R., Sun, X. Z., Joseph, P., Jaiswal, A. K., Zhang, D., Deng, P. S., and Chen, S. (1997) Catalytic properties of NAD(P)H: quinone oxidoreductase-2 (NQO2), a dihydronicotinamide riboside dependent oxidoreductase. *Arch. Biochem. Biophys. 347*, 221–228.

(24) Kwiek, J. J., Haystead, T. A., and Rudolph, J. (2004) Kinetic mechanism of quinone oxidoreductase 2 and its inhibition by the antimalarial quinolines. *Biochemistry 43*, 4538–4547.

(25) Mailliet, F., Ferry, G., Vella, F., Berger, S., Coge, F., Chomarat, P., Mallet, C., Guenin, S. P., Guillaumet, G., Viaud-Massuard, M. C., Yous, S., Delagrange, P., and Boutin, J. A. (2005) Characterization of the melatoninergic MT3 binding site on the NRH:quinone oxidoreductase 2 enzyme. *Biochem. Pharmacol. 71*, 74–88.

(26) Winger, J. A., Hantschel, O., Superti-Furga, G., and Kuriyan, J. (2009) The structure of the leukemia drug imatinib bound to human quinone reductase 2 (NQO2). *BMC Struct. Biol. 9*, 7.

(27) Dufour, M., Yan, C., Siegel, D., Colucci, M. A., Jenner, M., Oldham, N. J., Gomez, J., Reigan, P., Li, Y., Matteis, C. I. D., Ross, D., and Moody, C. J. (2011) Mechanism-based inhibition of quinone reductase 2 (NQO2). Selectivity for NQO2 over NQO1 and structural basis for flavoprotein inhibition. *ChemBioChem 12*, 1203–1208.

(28) Beall, H. D., Mulcahy, R. T., Siegel, D., Traver, R. D., Gibson, N. W., and Ross, D. (1994) Metabolism of bioreductive antitumor compounds by purified rat and human DT-diaphorases. *Cancer Res. 54*, 3196–3201.

(29) Friedlos, F., Jarman, M., Davies, L. C., Boland, M. P., and Knox, R. J. (1992) Identification of novel reduced pyridinium derivatives as synthetic co-factors for the enzyme DT diaphorase (NAD(P)H dehydrogenase (quinone), EC 1.6.99.2). *Biochem. Pharmacol. 44*, 25–31.

(30) Silverman, R. B. (1988) Mechanism based enzyme inhibition. In *Chemistry and Enzymology*, pp 3−30, CRC Press, Boca Raton, FL.

(31) Kitz, R., and Wilson, I. B. (1962) Esters of methanesulfonic acid as irreversible inhibitors of acetylcholinesterase. *J. Biol. Chem. 237*, 3245–3249.

(32) Lowry, O. H., Rosebrough, N. J., Farr, A. L., and Randall, R. J. (1951) Protein measurement with the Folin phenol reagent. *J. Biol. Chem. 193*, 265–275.

(33) Mosmann, T. (1983) Rapid colorimetric assay for cellular growth and survival: Application to proliferation and cytotoxicity assays. *J. Immunol. Methods 65*, 55–63.

(34) Brooks, B. R., Bruccoleri, R. E., Olafson, B. D., States, D. J., and Swaminathan, S. (1983) CHARMM: A program for macromolecular energy, minimization, and dynamics calculations. *J. Comput. Chem. 4*, 187–217.

(35) Luty, B. A., Wasserman, Z. R., Stouten, P. F. W., Hodge, C. N., Zacharias, M., and McCammon, J. A. (1995) A molecular mechanics/grid method for evaluation of ligand-receptor interactions. *J. Comput. Chem. 16*, 454–464.

(36) Gilson, M. K., and Honig, B. (1988) Calculation of the total electrostatic energy of a macromolecular system: Solvation energies, binding energies, and conformational analysis. *Proteins 4*, 7–18.

(37) Reigan, P., Colucci, M. A., Siegel, D., Chilloux, A., Moody, C. J., and Ross, D. (2007) Development of indolequinone mechanism-based inhibitors of NAD(P)H:quinone oxidoreductase 1 (NQO1): NQO1 inhibition and growth inhibitory activity in human pancreatic MIA PaCa-2 cancer cells. *Biochemistry 46*, 5941–5950.

(38) Nolan, K. A., Zhao, H., Faulder, P. F., Frenkel, A. D., Timson, D. J., Siegel, D., Ross, D., Burke, T. R., Jr., Stratford, I. J., and Bryce, R. A. (2007) Coumarin-based inhibitors of human NAD(P)H:quinone oxidoreductase-1. Identification, structure-activity, off-target effects and in vitro human pancreatic cancer toxicity. *J. Med. Chem. 50*, 6316–6325.

(39) Cavelier, G., and Amzel, L. M. (2001) Mechanism of NAD(P)H:quinone reductase: Ab initio studies of reduced flavin. *Proteins 43*, 420–432.

(40) Zhou, Z., Fisher, D., Spidel, J., Greenfield, J., Patson, B., Fazal, A., Wigal, C., Moe, O. A., and Madura, J. D. (2003) Kinetic and docking studies of the interaction of quinones with the quinone reductase active site. *Biochemistry 42*, 1985–1994.

(41) Suleman, A., and Skibo, E. B. (2002) A comprehensive study of the active site residues of DT-diaphorase: Rational design of benzimidazolediones as DT-diaphorase substrates. *J. Med. Chem. 45*, 1211–1220.

(42) Maiti, A., Reddy, P. V., Sturdy, M., Marler, L., Pegan, S. D., Mesecar, A. D., Pezzuto, J. M., and Cushman, M. (2009) Synthesis of casimiroin and optimization of its quinone reductase 2 and aromatase inhibitory activities. *J. Med. Chem. 52*, 1873–1884.

(43) Colucci, M. A., Reigan, P., Siegel, D., Chilloux, A., Ross, D., and Moody, C. J. (2007) Synthesis and evaluation of 3-aryloxymethyl-1,2-dimethylindole-4,7-diones as mechanism-based inhibitors of NAD(P)H:quinone oxidoreductase 1 (NQO1) activity. *J. Med. Chem. 50*, 5780–5789.